

ACCEPTED MANUSCRIPT

A systemic view on the distribution of diet-derived methanol and hepatic acetone in mice

To cite this article before publication: Martin Kistler *et al* 2017 *J. Breath Res.* in press <https://doi.org/10.1088/1752-7163/aa8a15>

Manuscript version: Accepted Manuscript

Accepted Manuscript is “the version of the article accepted for publication including all changes made as a result of the peer review process, and which may also include the addition to the article by IOP Publishing of a header, an article ID, a cover sheet and/or an ‘Accepted Manuscript’ watermark, but excluding any other editing, typesetting or other changes made by IOP Publishing and/or its licensors”

This Accepted Manuscript is © 2017 IOP Publishing Ltd.

During the embargo period (the 12 month period from the publication of the Version of Record of this article), the Accepted Manuscript is fully protected by copyright and cannot be reused or reposted elsewhere.

As the Version of Record of this article is going to be / has been published on a subscription basis, this Accepted Manuscript is available for reuse under a CC BY-NC-ND 3.0 licence after the 12 month embargo period.

After the embargo period, everyone is permitted to use copy and redistribute this article for non-commercial purposes only, provided that they adhere to all the terms of the licence <https://creativecommons.org/licenses/by-nc-nd/3.0>

Although reasonable endeavours have been taken to obtain all necessary permissions from third parties to include their copyrighted content within this article, their full citation and copyright line may not be present in this Accepted Manuscript version. Before using any content from this article, please refer to the Version of Record on IOPscience once published for full citation and copyright details, as permissions will likely be required. All third party content is fully copyright protected, unless specifically stated otherwise in the figure caption in the Version of Record.

View the [article online](#) for updates and enhancements.

A systemic view on the distribution of diet-derived methanol and hepatic acetone in mice

Martin Kistler^{1,2,5,*}, Andreea Muntean^{2,3,6,7,*}, Vera Höllriegl³, Georg Matuschek³, Ralf Zimmermann^{6,7},
Christoph Hoeschen⁴, Martin Hrabě de Angelis^{1,2,5,8} and Jan Rozman^{1,2,5,+}

¹Institute of Experimental Genetics, Helmholtz Zentrum München, German Research Centre for Environmental Health, Ingolstädter Landstrasse 1, 85764 Neuherberg, Munich, Germany

²German Mouse Clinic, Institute of Experimental Genetics, Helmholtz Zentrum München, German Research Centre for Environmental Health, Ingolstädter Landstrasse 1, 85764 Neuherberg, Munich, Germany

³Institute of Radiation Protection, Helmholtz Zentrum München, German Research Center for Environmental Health, Ingolstädter Landstrasse 1, 85764 Neuherberg, Munich, Germany

⁴Institute of Medical Systems Technology, Otto-von-Guericke-University, P.O.Box 4120, 39016 Magdeburg

⁵German Centre for Diabetes Research (DZD)

⁶Joint Mass Spectrometry Centre - Cooperation Group "Comprehensive Molecular Analytics", Helmholtz Zentrum München, German Research Center for Environmental Health, Ingolstädter Landstrasse 1, 85764 Neuherberg, Munich, Germany

⁷Institute of Chemistry, University of Rostock, 18051 Rostock, Germany

⁸Chair for Experimental Genetics, Life and Food Science Center Weihenstephan, Technische Universität München, 85354 Freising-Weihenstephan, Germany

*Contributed equally to the manuscript

+Corresponding author: Phone: +49 89 3187 3807; E-mail: jan.rozman@helmholtz-muenchen.de (J. Rozman), Postal: Institute of Experimental Genetics, Helmholtz Zentrum München, German Research Center for Environmental Health, Ingolstädter Landstrasse 1, 85764 Neuherberg, Munich, Germany

Abbreviations: VOCs, volatile organic compounds; LFD low fat diet; PTR-MS, proton transfer reaction mass spectrometry; TOF, time of flight; pk, peak;

35 **Abstract**

36

37 Volatile organic compounds (VOCs) from breath can successfully be used to diagnose disease-
38 specific pathological alterations in metabolism. However, the exact origin and underlying biochemical
39 pathways that could be mapped to VOC signatures are mainly unknown. There is a knowledge gap
40 regarding the contribution of tissues, organs, the gut microbiome, and exogenous factors to the “sum
41 signal” from breath samples. Animal models for human disease such as mutant mice provide the
42 possibility to reproduce genetic predisposition to disease, thereby allowing the in-depth analysis of
43 metabolic and biochemical functions. We hypothesized that breath VOCs can be traced back to
44 origins and organ-specific metabolic functions by combining breath concentrations with systemic
45 levels detected in different organs and biological media (breath, blood, feces and urine). For this we
46 fed C57Bl/6N mice a grain-based chow or a purified low-fat diet, thereby modifying the emission of
47 methanol in breath whereas acetone levels were unaffected. We then measured headspace
48 concentrations of both VOCs in ex-vivo samples of several biological media. Especially cecum
49 content was identified as a likely source of systemic methanol, whereas liver showed highest acetone
50 concentrations. Our findings are a first step to the systemic mapping of VOC patterns to metabolic
51 functions in mice because differences between VOCs could be traced to different sources in the body.
52 As a future aim, different levels of so-called omics technologies (genomics, proteomics,
53 metabolomics, and breathomics) could be mapped to metabolic pathways in multiple tissues
54 deepening our understanding of VOC metabolism and possibly leading to early non-invasive
55 biomarkers for human pathologies.

56

Accepted Manuscript

1. Introduction

Volatile organic compounds (VOCs) measured in exhaled breath have been shown to provide information about metabolic state and disease in humans as well as in model organisms for human diseases. Breath analysis has the potential of being used as a reliable, low cost and easy-to-use method to classify healthy and diseased subjects in a number of pathologies (Baranska et al., 2016; Fernández del Río et al., 2015; Nakhleh et al., 2016; Obermeier et al., 2017; van Vliet et al., 2017). Closer investigations revealed that breath VOCs are derived from a combination of various exogenous and endogenous sources (Lindinger et al., 1997; Pleil et al., 2013). This is a major reason why the physiological link between VOC signatures and disease metabolism is poorly understood. While uptake from the environment, or food and beverages reflect the exposome, endogenous VOCs originate from either endogenous metabolic processes or the individual microbial metabolism. Both, changes in the metabolic status and modified composition of the microbiome may reflect or interact with disease. Thus, dissection of the origin of single VOCs from different organs, tissues and metabolic pathways is important to improve the robustness of the method and its usefulness to provide early biomarkers for disease. In the field of VOC analytics, several attempts were made to better understand which processes lead to altered VOC metabolism. For such approaches, stable isotope labelled substrates were administered in mice to follow up specific VOCs (Sinues et al., 2017). In humans, enzyme functions were monitored in vivo (Ruzsanyi et al., 2014). Other studies addressed the relation between blood and breath in humans (O'Hara et al., 2009), analysed VOC emissions from single cell lines (Brunner et al., 2010; Filipiak et al., 2016), from tissue samples (Filipiak et al., 2014) or (pathogenic) microbiota (Bean et al., 2016). A complete view on organ and tissue concentrations of external or endogenous VOCs is required to better understand the origin of VOCs. This can help to map VOCs to specific metabolic functions. Evidently mammalian model organisms such as laboratory rats or the C57BL/6N mouse facilitated pilot work in this field (Aprea et al., 2012; Hüppe et al., 2016; Kistler et al., 2016; Sinues et al., 2017; Szymczak et al., 2014).

We investigated systemic VOC distribution in organs, blood, feces, urine, and breath of male C57BL/6N mice that were fed a purified low fat experimental diet or standard laboratory chow. For this study, we selected methanol, a VOC modified by diet and found in breath after ingestion of fruits, vegetables, alcoholic or aspartame sweetened beverages (Lindinger et al., 1997; Španěl et al., 2015). We previously found it elevated in exhaled breath of mice in response to feeding a grain-based chow diet compared to a purified control diet (Kistler et al., 2014). Acetone, a better studied endogenous metabolite selected as second compound. We hypothesized that breath signals of both compounds can be linked to headspace concentrations from several mouse tissues and media like urine, blood, feces, and cecum content. By using such a system-wide approach, the so far largely unexplored links

92 between several tissues and VOCs that finally contribute to the sum signal presented in breath can be
93 investigated and mapped to metabolic functions.

94 2. Material and Methods

96 2.1. Animal housing and diet regimes

97 Male mice (n = 34) were housed in type IIL polycarbonate cages with individual ventilation
98 (Tecniplast, Italy) in specific pathogen-free conditions at the German Mouse Clinic (GMC) (Fuchs et
99 al., 2009). Air humidity of 50-60% and a 12:12 light/dark cycle were maintained. Wood shavings
100 were used for bedding (Altromin GmbH, Germany). All mice had *ad libitum* access to pelleted
101 laboratory chow (no. 1314, Altromin, Lage, Germany) and drinking water from weaning on. From the
102 age of 32 weeks on mice were randomly assigned to either continued chow diet feeding or a semi-
103 purified low fat diet (low fat: E 15000-04, Ssniff, Soest, Germany) for a period of 3 weeks until the
104 VOC analysis measurements were conducted. All experiments were performed following animal
105 welfare regulations supervised by the district government of Upper Bavaria (Regierung von
106 Oberbayern).

107 Analysis of VOCs from *ad libitum* fed mice was performed between 7 am and 1 pm. Mice were in a
108 postprandial state as they typically feed in the early morning hours. Chow and LFD mice were
109 measured in alternating order to remove potential systemic bias. Mice were weighed immediately
110 before the VOC measurement to the nearest 0.1 g.

112 2.2. Proton-transfer reaction time-of-flight mass spectrometry

113 A high-sensitivity Proton Transfer Reaction Mass Spectrometer (PTR-MS, Ionicon Analytic GmbH,
114 Innsbruck, Austria) with a resolution of $m/\Delta m \leq 2000$ was used. Settings and machine parameters
115 were applied as described previously (Kistler et al., 2016). The following deviations were made: A
116 mass range from m/z 0 to 356 was recorded and the sum spectra were stored with integration time of 1
117 s (TOF-DAQ, Tofwerk AG, Switzerland). Calibration was performed using known peaks $\text{H}_3^{18}\text{O}^+$ (m/z
118 21.0221), NO^+ (m/z 29.9971), and the 2 high mass peaks provided by the built-in PerMaSCal unit
119 $\text{C}_6\text{H}_5\text{I}^+$ (m/z 203.9431) and $\text{C}_6\text{H}_5\text{I}_2^+$ (m/z 330.8481). A total of 306 peaks were selected manually from
120 the spectra using PTR-MS Viewer (Version 3.2.1.2, Ionicon analytic GmbH, Innsbruck, Austria).

121 2.3. Real-time VOC analysis in unrestrained and anaesthetized mice

122 A setup and protocol for real-time measurement of VOCs in unrestrained mice using respiratory
123 chambers was again applied as described previously (Kistler et al., 2016, 2014; Szymczak et al.,

1
2
3 124 2014). In brief, a polypropylene box (volume 600 mL) was connected to a proton transfer time-of-
4
5 125 flight mass spectrometer (PTR-TOF-MS) and to a gas supply of synthetic air (20% oxygen, 80%
6
7 126 nitrogen, concentration of hydrocarbons 0.1 ppm, Linde AG, Germany). After flushing with synthetic
8
9 127 air, blank samples were drawn from the empty chamber to control for leakage (5 min, flow 60 mL
10
11 128 min⁻¹ controlled by PTR). During a second flushing with synthetic air, the mouse was placed into the
12
13 129 respirometry chamber and the accumulation of exhaled VOCs was monitored. Flushing (2 min, flow 3
14
15 130 L h⁻¹) and accumulation of VOCs (5 min, flow 60 mL min⁻¹ controlled by PTR) were repeated three
16
17 131 times each. Air drawn from the chamber by the PTR was replenished from a Teflon bag reservoir
18
19 132 filled with synthetic air (capacity of 10 L, Welch Fluorocarbon Inc., Dover, USA) connected to the
20
21 133 chamber.

22
23 134 In addition to VOC measurements using mice in a chamber, we aimed to verify that methanol and
24
25 135 acetone signals were mainly breath driven. Thus, we obtained breath data using a nose mask similar to
26
27 136 previously published studies using rats (Aprea et al., 2012). In brief, a 15 ml falcon tube was
28
29 137 shortened to a volume of 4 ml. The end of the tube was connected to the PTR using PTFE tubing. For
30
31 138 the replacement of withdrawn gas, a 1 mm hole was placed at the side of the tube to allow steady
32
33 139 airflow. A subgroup of anaesthetized mice (13 per group, i.p. injection of 100 mg/kg bodyweight
34
35 140 ketamine and 10 mg/kg bodyweight xylazine) were measured twice for more than 20s. Surrounding
36
37 141 room air was monitored both before and after breath measurements.

38
39 142

37 143 *2.4. Organ sampling, pre-processing and head space measurement*

38 144 Blood from anesthetised mice was sampled from the orbital sinus. Coagulation was inhibited by
39
40 145 sampling directly into EDTA-containing tubes, which were immediately shock-frozen in liquid
41
42 146 nitrogen. After blood sampling, abdominal cavity was opened and the following organs and samples
43
44 147 were taken: gastric, duodenal and cecum content; quadriceps femoris muscle, peri-renal white adipose
45
46 148 tissue, kidney, liver, lung, heart, spleen, testis, whole brain. Urine and feces samples were collected
47
48 149 from the respirometry box while breath samples were collected. Samples were shock-frozen in liquid
49
50 150 nitrogen immediately after dissection. Samples were analysed within two weeks of storage at -80 °C.

51 151 For analysis of VOCs emitted, samples (except blood and urine) were homogenized (Tissue Lyzer
52
53 152 MM400, Retsch GmbH, Haan, Germany). For this, pre-cooled steel balls were added to the sample
54
55 153 tube and tubes were placed in a holder pre-frozen in liquid nitrogen. Homogenization was performed
56
57 154 using a shaking frequency of 30 Hz for 2.5 minutes. A targeted mass of 250 mg homogenate was
58
59 155 transferred to a glass vial, flushed with synthetic air and incubated for 3 minutes at 37 °C. Samples of
60
156 organs with physiologically low mass (e.g. heart, lung, spleen, testes) or variable availability (e.g.
157 urine, feces, gut content) were excluded if below 50 mg. In total, headspace of 516 samples was
158 measured using a PTR-TOF-MS; extracted gas volume was replaced by synthetic air.

159 2.5. Data analysis and statistics

160 2.5.1. Calculation of VOC source strengths and concentrations

161 The source strength in ppb ml/min was derived by applying a compartment model on the recorded
162 saturation curves (non-linear regression, described in (Szymczak et al., 2014)) and data pre-
163 procession was performed as described previously if not stated otherwise (Kistler et al., 2016, 2014).
164 The concentration used for further analysis was determined using a mean of two maximal values.
165 Outliers (defined as greater than four standard deviations from mean) were removed. Nose
166 measurements were differentially corrected against room air background.

167 2.5.2. Statistics and data visualization

168 For the analysis of diet-induced effects on the VOC source strengths and concentrations, linear
169 models were applied. Data were log-transformed to approximate a normal distribution (tested visually
170 by qq-plotting). The variance between groups was controlled using both boxplots of source strength as
171 well as residuals and residual versus fitted data plots. As a larger number of tests leads to summation
172 of Type I – error, control of false discovery rate after Benjamini and Hochberg (Benjamini and
173 Hochberg, 1995) was applied and all p-values were adjusted according to a 10% FDR.

174 Principal component analysis of scaled and centred data was performed using R. Boxplots were
175 created using the R package *ggplot2* using means of maximal headspace concentrations and source
176 strength data (Wickham, 2009). As a complete data-matrix is required to calculate the correlation
177 plots, missing data was imputed using the *mice* R package (Buuren and Groothuis-Oudshoorn,
178 2011), which accounted for 3.024% of data. Correlation plots were performed using the R package
179 *corrplot* (pearson correlations).

180

181 3. Results

182

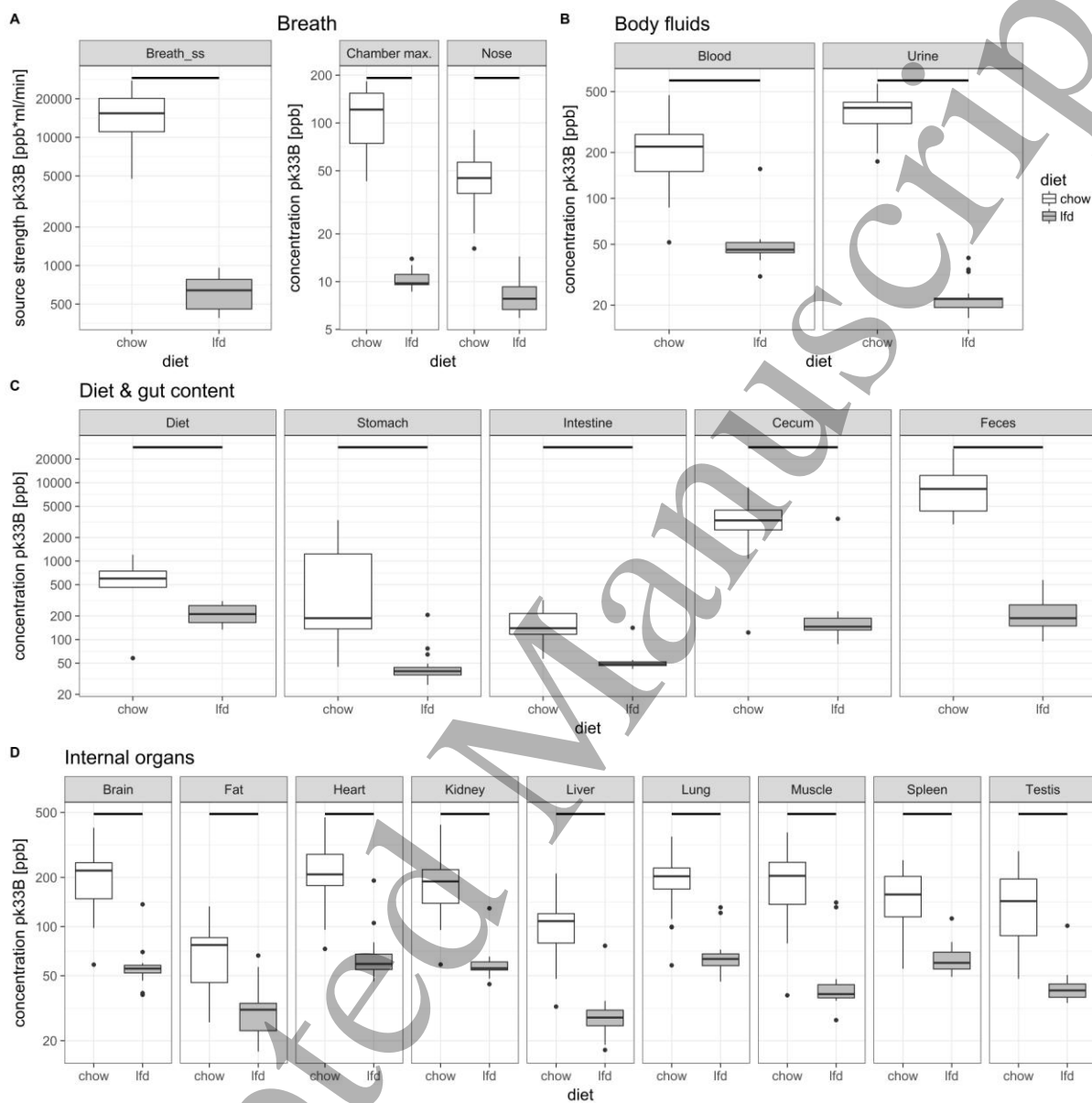
183 3.1. Elevation in systemic methanol levels might be driven by cecum methanol release

184

185 Emission of methanol was increased in chow fed mice both in source strength in breath as well as in
186 maximum headspace concentration of all organ and media samples during the measurement (Figure
187 1A). As a next step, we followed up on whether a difference in concentrations of the selected exhaled
188 VOCs induced by a diet change can be recovered from the respective headspace concentrations of
189 individual organ samples. A similar increase in the chow group was present in blood and, even more
190 pronounced, in urine (Figure 1B). When following the digestive tract, methanol levels increased

191 tenfold from stomach to cecum (Figure 1C). In all internal organs, higher methanol headspace
 192 concentrations could be detected in chow fed mice (Figure 1D).

193



194

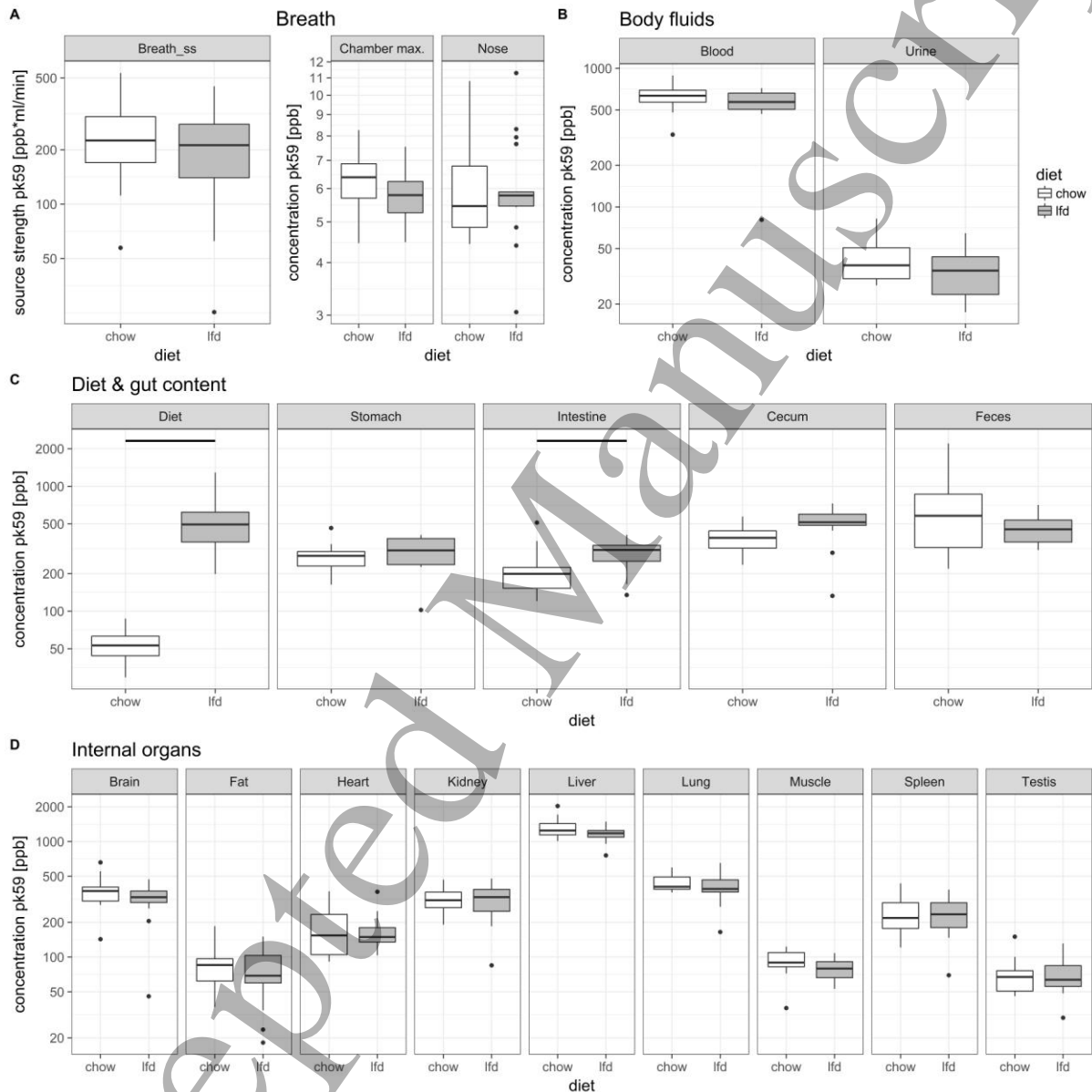
195 **Figure 1: Methanol concentrations from tissue homogenate headspaces.** Mice fed either chow (white, n = 17) or LFD
 196 (grey, n = 17). Methanol breath source strength, maximal concentration during mouse measurement and nose mask
 197 measurements for a subset (both n = 13) are shown in A. Headspace concentrations of blood and urine are shown in B. Diet,
 198 stomach, intestine and cecum content and feces head space concentrations are shown in C. Headspace concentrations of
 199 brain, fat, heart, kidney, liver, lung, muscle, spleen and testis are shown in D.

200

201 3.2. Liver is a major site of acetone release

202 In contrast to methanol, acetone levels were comparable between groups after the diet change both in
 203 breath source strength as well as in maximum headspace concentration (Figure 2 A). No significant

204 difference could be detected in body fluids (Figure 2 B). When following the digestive tract, a slight
 205 increase could be observed in the content of the intestine (Figure 2 C). No major diet effect was found
 206 in the acetone concentration detected in any internal organs. Hepatic tissue homogenates showed
 207 highest acetone concentrations in headspace, brain, heart, kidney, lung, and spleen were intermediate.
 208 Lowest values were detected in white adipose tissue, muscle and testes (Figure 2 D).



210

211 **Figure 2: Acetone concentrations from various tissue homogenate headspaces.** Mice fed either chow (white, n = 17) or
 212 LFD (grey, n = 17). Acetone breath source strength, maximal concentration during mouse measurement and nose mask
 213 measurements for a subset (both n = 13) are shown in A. Headspace concentrations of blood and urine are shown in B. Diet,
 214 stomach, intestine and cecum content and feces head space concentrations are shown in C. Headspace concentrations of
 215 brain, fat, heart, kidney, liver, lung, muscle, spleen and testis are shown in D.

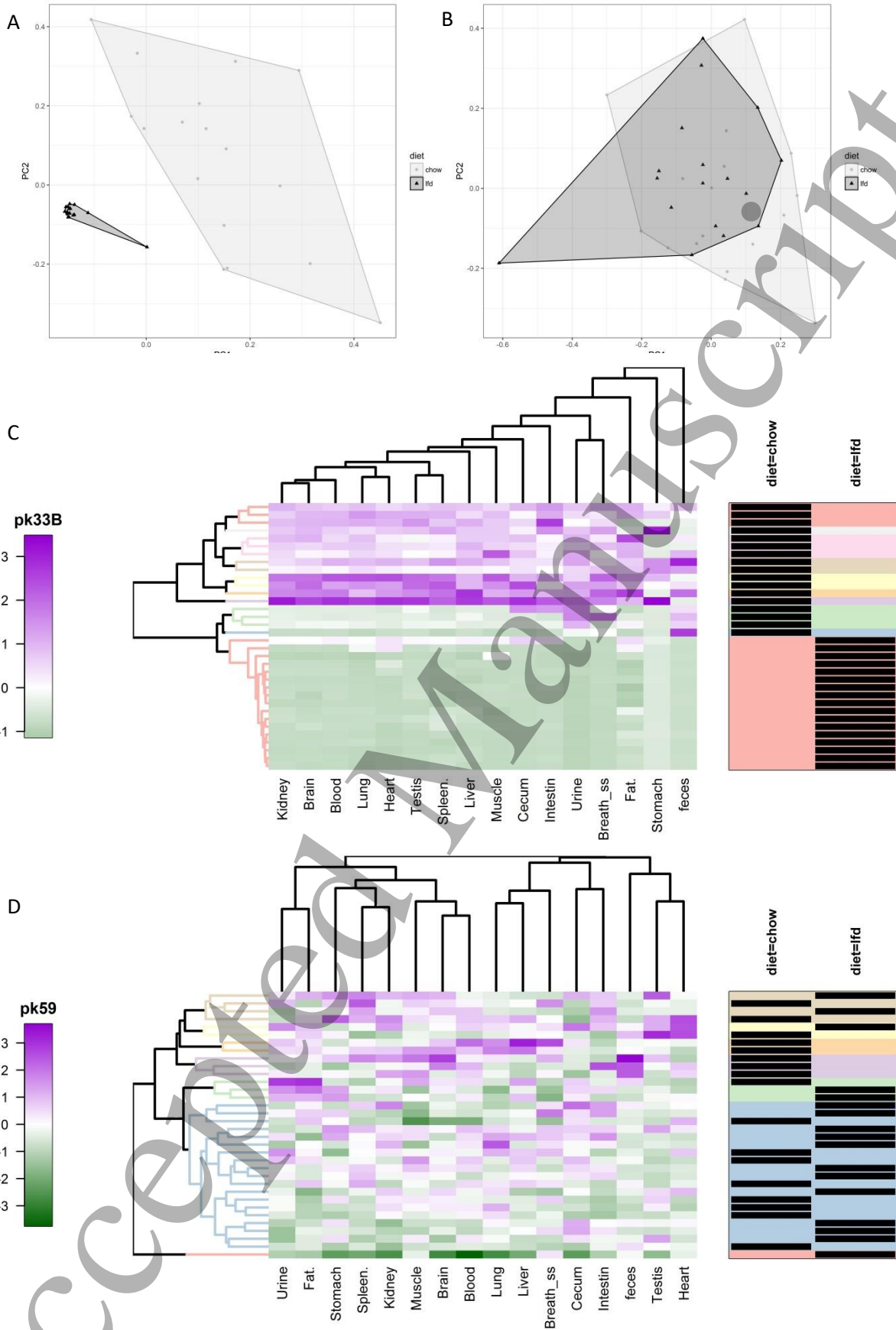
216

1
2
3 217 *3.3. Methanol levels of tissue samples and media cluster by diet-interventions*
4
5 218

6
7 219 Next we used unsupervised clustering methods to determine whether groups clustered by diet.
8
9 220 Methanol levels in all samples were clearly separated by diet as we could show by principle
10
11 221 component analysis (Figure 3A) and hierarchical clustering (Figure 3C). In contrast, acetone levels in
12
13 222 different media were not separated by diet both in PCA and hierarchical clustering (Figure 3B and D).
14
15 223

16
17
18
19
20
21
22
23
24
25
26
27
28
29
30
31
32
33
34
35
36
37
38
39
40
41
42
43
44
45
46
47
48
49
50
51
52
53
54
55
56
57
58
59
60

Accepted Manuscript



224

225

226

1
2
3
4
5
6
7
8
9
10
11
12
13
14
15
16
17
18
19
20
21
22
23
24
25
26
27
28
29
30
31
32
33
34
35
36
37
38
39
40
41
42
43
44
45
46
47
48
49
50
51
52
53
54
55
56
57
58
59
60

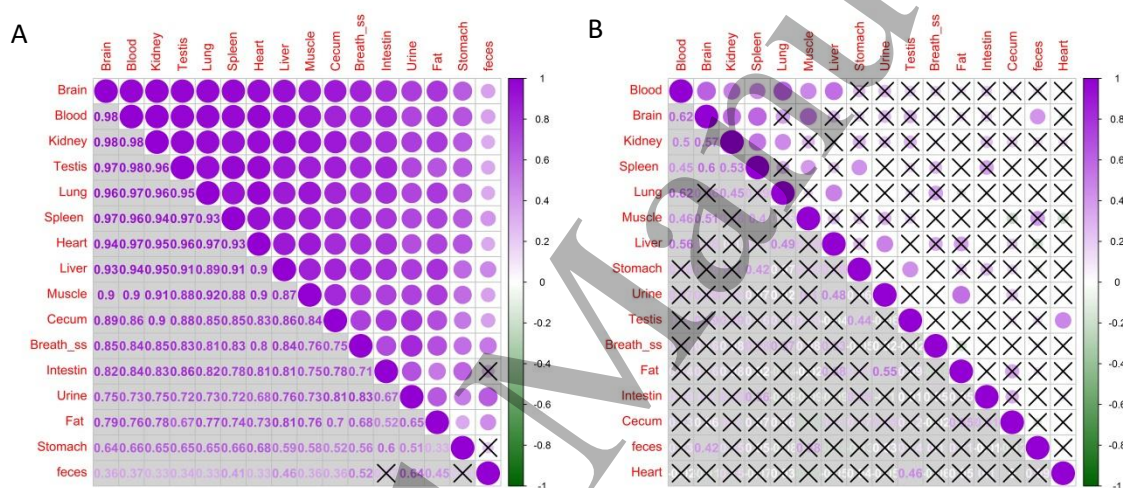
ACCEPTED MANUSCRIPT

227 **Figure 3: Principal component analysis (PCA) and heatmaps with hierarchical clustering of emissions from various**
 228 **tissues and samples.** Components one and two of a PCA of main methanol signal at 33.05 (A, pk33B) or main acetone
 229 signal at 59.05 (B, pk59) are shown for stomach, intestine and cecum content, feces, liver, heart, lung, brain, muscle, spleen,
 230 testis, fat, blood, urine and source strength in breath from mice fed either chow (white, n = 17) or LFD (grey, n = 17).
 231 Heatmaps of methanol (C) and acetone (D) data are shown with hierarchical clustering of individual mice (mean data, rows,
 232 sub-clusters colored) and tissue and media samples (columns). Data is scaled and centered. Color-coding legend shown on
 233 the left. Classification of individual mice is annotated on the right (diet = chow or low fat (lfd)).

234

235 3.4. Methanol concentrations are highly correlated in internal organs and blood

236 Methanol concentrations in the headspace of different media were highly positively correlated
 237 especially within the internal organs and blood (Figure 4 A). In contrast, acetone concentrations in the
 238 same media samples showed fewer significant and generally weaker correlations.



239

240 **Figure 4: Correlation matrix ordered after first principal component.** Pearson correlations between headspace
 241 concentrations of main methanol signal at 33.05 (A, pk33B) or main acetone signal at 59.05 (B, pk59) are shown for
 242 stomach, intestine and cecum content, faeces, liver, heart, lung, brain, muscle, spleen, testis, fat, blood, urine and source
 243 strength in breath from mice fed either chow (white, n = 17) or LFD (grey, n = 17). Correlation strength is color-coded and
 244 shown in circle size (upper half) as well as absolute coefficients (lower half). Non-significant correlations are marked with a
 245 cross.

246

247 4. Discussion

248

249 In this study we compared the distributions of mostly dietary modified methanol with endogenously
 250 produced acetone through a series of gastro-intestinal contents, organ lysates and body fluids. As
 251 shown earlier, feeding mice a grain-based chow diet in comparison to a purified diet that only
 252 contains synthetic ingredients increases emitted levels of methanol (Kistler et al., 2014). Interestingly,

1
2
3 253 this did not only hold true for breath methanol but the difference can be replicated in every tissue,
4
5 254 fluid and biomaterial investigated in this study. In addition, principal component analysis and
6
7 255 hierarchical clustering clearly separated samples from mice fed a chow diet from LFD mice.
8
9 256 Exemplarily, we selected acetone, a well-studied endogenous VOC where breath emission is not
10
11 257 influenced by dietary matrix change. As expected from breath data, no diet related differences could
12
13 258 be detected in organs selected for headspace analysis as well. Therefore, we show that systemic
14
15 259 changes of VOCs can be detected with this approach.

16 260 We hypothesized in our previous study that methanol production depends on microbial activity in the
17
18 261 gastro-intestinal tract. This was further substantiated by the fact that upon overnight food restriction
19
20 262 (and thus microbial substrate restriction), methanol levels are reduced (Kistler et al., 2016). When
21
22 263 following the diet and gastro-intestinal content through the digestive system, a massive ~10 fold
23
24 264 increase in methanol concentrations can be found beginning in cecum. It is well known that microbial
25
26 265 density increases towards the lower digestive tract to up to 10^{12} organisms per gram (Hooper and
27
28 266 Gordon, 2001). Methanol is a ubiquitous compound present in the breath of humans and other
29
30 267 mammals (Eriksen *et al*, 1963). For a long time, it was considered to be exclusively due to exogenous
31
32 268 production after ingestion of fruits, vegetables, alcoholic or aspartame sweetened beverages
33
34 269 (Lindinger *et al*, 1997). Therefore, it is very likely that methanol release is linked to the metabolism of
35
36 270 the gut microbiome. Interestingly, there is also literature about genuine endogenous methanol release,
37
38 271 for example from carboxy methylated proteins, which can be freed by carboxymethylase (Diliberto
39
40 272 and Axelrod, 1976, 1974) or under neutral or basic conditions, or from S-adenosyl methionine (SAM)
41
42 273 (Axelrod and Daly, 1965). However, our data suggested that exogenous sources seem to dominate
43
44 274 systemic levels. Interestingly, acetone concentrations, which are not affected by diet, tissue
45
46 275 headspaces detected in both groups were remarkably comparable and reproducible. We assume that
47
48 276 the tissue with the highest headspace concentration is a likely candidate for the endogenous
49
50 277 production of acetone. Highest levels could be found in liver tissue. This is well in accordance with
51
52 278 published work about acetone metabolism, as liver is the major site of ketogenesis. Acetone can be
53
54 279 derived from the other ketone bodies aceto-acetate and indirectly from beta-hydroxybutyrate
55
56 280 (Puchalska and Crawford, 2017). Thus, according to these two examples information about the origin
57
58 281 of certain targeted VOCs can be gained by this methodology.

59
60 282 Remarkably, using this method of sampling from various parts of the organism, interesting
283
284 283 distributions in the two selected VOCs can be detected. In methanol, we found a high correlation of
285
286 284 levels in the internal organs, which is reduced but still relatively high in other samples. Internal organs
287
288 285 are linked by blood as a transfer compartment, and after gastro-intestinal uptake of methanol the
286
287 286 blood circulation is the major route of distribution through the body. Interestingly, the solubility of
288
289 287 methanol in blood and lean tissues is similar (Fiserova-Bergerova, 1985), which is in accordance with
290
291 288 similar headspace concentrations in blood and lean tissues. In addition a reduction in methanol levels

1
2
3 289 could be found in fat and liver tissue. Existing pharmacokinetic models of methanol exposure via
4
5 290 inhalation typically differentiate between liver as the metabolic clearance compartment, kidney for
6
7 291 excretion, and richly or slowly perfused organs (Fiserova-Bergerova, 1985; Fiserova-Bergerova and
8
9 292 Diaz, 1986; Horton et al., 1992; Paterson and Mackay, 1989; Ward et al., 1997). The perfusion of
10
11 293 adipose tissue is significantly less compared to other organs and depends on the physical activity of
12
13 294 the exanimated models (Fiserova-Bergerova, 1985). Moreover, the fat-gas partition coefficient and
14
15 295 the large difference in the methanol solubility of the slowly perfused fat compared to lean tissues
16
17 296 explain the corresponding reduced level (Paterson and Mackay, 1989).

18
19 297 Similar to fat, reduced methanol levels were observed in the liver as well. The hepatic tissue is not
20
21 298 only a richly blood-perfused tissue, but it is one of the most metabolically active tissues in the body. It
22
23 299 is known that the degradation of methanol primarily occurs in the hepatic tissue (96.9 % vs. 0.6% via
24
25 300 urine and 2.5% via breath) which might explain lower observed ex-vivo levels (Skrzydewska, 2003).
26
27 301 Furthermore the clearance of methanol via urine might be indicated by the increase of methanol from
28
29 302 blood to urine samples in chow feed mice. In LFD fed mice, absolute levels in urine are reduced by
30
31 303 tendency, which could be explained if methanol is reabsorbed (actively) from primary urine. This
32
33 304 leads to the hypothesis that there exists a physiological set point, pointing out potential physiological
34
35 305 roles for methanol (Dorokhov et al., 2015). In contrast to methanol, acetone urine levels are reduced
36
37 306 compared to blood levels in both groups. As acetone contains metabolizable energy, it is reabsorbed
38
39 307 from primary urine. This is especially true in ad libitum fed conditions, when ketone body
40
41 308 concentrations are low in comparison to fasted or other ketogenic states where the reabsorption
42
43 309 capacity is overcome (Puchalska and Crawford, 2017). Regarding acetone, concentrations in different
44
45 310 samples were generally weaker correlated (Figure 4b). Since there is no dedicated intervention, *ad*
46
47 311 *libitum* fed acetone levels vary less than methanol levels (due to the intervention), and physiological
48
49 312 situations like fasting might be an interesting future experiment to perform in combination with this
50
51 313 methodology. Despite the high concentrations in liver headspace there seems to be a typical pattern
52
53 314 very similar in both feeding groups, indicating that something like an organ specific VOC-signature
54
55 315 might exist.

56
57 316 When studying methanol metabolism, differences in methanol degradation between rodents and
58
59 317 primates need to be taken into account. Degradation of methanol to formaldehyde and further
60
318 metabolites in rodents is primarily performed by the enzyme catalase, whereas in contrast primates
319 use alcohol dehydrogenase and cytochrome P2E1 (Sweeting et al., 2010). Furthermore, formate
320 detoxification in primates is limited by folate availability, leading to accumulation and intoxication to
321 which rodents are not prone. As a consequence, methanol is cleared much faster than in humans. Still,
322 in this study, it can be seen in mouse tissue samples after mice consumed chow food presumably
323 hours before. Another interesting question is to what extent remaining blood in the organs could
324 contribute to the observed levels. For other biological questions, protocols for e.g. saline perfusion to

1
2
3 325 remove blood from tissues are established. To our knowledge, no study has shown or systematically
4
5 326 evaluated the effect of such procedures to the remaining VOC content, the effects and usefulness of
6
7 327 perfusion need to be addressed in further studies. In addition to the question of potential saline
8
9 328 perfusion discussed above, for several aspects of the methodology other options can be discussed. In
10
11 329 the performed protocol, we aimed to optimize the procedure for speed, thus minimizing the time for
12
13 330 VOC losses due to emission from organs or (bio-) chemical spontaneous or enzyme-mediated
14
15 331 processes. As such, no perfusion was performed, since time from killing the mouse to shock freezing
16
17 332 in liquid nitrogen would have been doubled at least. In addition, we decided to homogenize the tissue
18
19 333 in a frozen state. By destroying tissue organisation, VOC release can be increased with reduced
20
21 334 gradients through the sample. However, other groups have used complete tissue or complete and
22
23 335 “chewed” food samples for headspace analysis of VOCs (Farneti et al., 2017; Filipiak et al., 2014). It
24
25 336 might depend on the question of interest which sample preparation is feasible.

26 337

27 338 **5. Conclusion and perspective**

28
29 339 In the presented work we showed that by using dietary modification of a VOC and measuring breath
30
31 340 in combination with an ex-vivo headspace of organs approach, information about volatile distribution
32
33 341 and physiology can be gained as shown in two well-studied proof of principle VOCs. By applying this
34
35 342 method, the origin and metabolism of unknown breath VOCs can be studied. Furthermore,
36
37 343 understanding the contribution of single organ systems to breath levels can be instrumental for
38
39 344 alternative diagnosis of organ pathologies in the clinics. In combination with different levels of so-
40
41 345 called omics technologies (genomics, proteomics, metabolomics, and breathomics), a multi-organ
42
43 346 view could contribute to map metabolic pathways and origins of VOCs.

44 347

45 348 **6. Author contributions**

46 349

47
48 350 M. K. conceived and designed the experiments, reviewed and analysed data and wrote, reviewed and
49
50 351 edited the manuscript.

51
52 352 A.M. researched data, reviewed data and wrote, reviewed and edited the manuscript.

53
54 353 G.M., V.H., C.H., R.Z. and M.H.A. contributed to discussion, reviewed and edited the manuscript.

55
56 354 J.R. conceived and designed the experiments, reviewed data, wrote, reviewed and edited the
57
58 355 manuscript.

1
2
3 356
4
5
67 357 **Acknowledgments**8 358
9
10

11 359 The authors declare that they have no conflict of interest. We thank Ann Elisabeth Schwarz and all
12 360 animal caretakers in the GMC for their technical contribution to mouse care and phenotyping and
13 361 Chris Mayhew (Institute for Breath Research, University of Innsbruck) for proofreading of the
14 362 manuscript. This work was partly funded by the FP7 Marie Curie Initial Training Network PIMMS
15 363 (Grant Agreement No. 287382), by the German Center for Diabetes Research (DZD) and by German
16 364 Federal Ministry of Education and Research (Infrafrontier grant 01KX1012).

17
18
19
20
21
22 365
23
24
25
26
27
28
29
30
31
32
33
34
35
36
37
38
39
40
41
42
43
44
45
46
47
48
49
50
51
52
53
54
55
56
57
58
59
60

Accepted Manuscript

366 7. References

- 367
- 368 Aprea, E., Morisco, F., Biasioli, F., Vitaglione, P., Cappellin, L., Soukoulis, C., Lembo, V., Gasperi,
369 F., D'Argenio, G., Fogliano, V., Caporaso, N., 2012. Analysis of breath by proton transfer
370 reaction time of flight mass spectrometry in rats with steatohepatitis induced by high-fat diet.
371 *J. Mass Spectrom.* JMS 47, 1098–1103. doi:10.1002/jms.3009
- 372 Axelrod, J., Daly, J., 1965. Pituitary gland: enzymic formation of methanol from S-
373 adenosylmethionine. *Science* 150, 892–893.
- 374 Baranska, A., Mujagic, Z., Smolinska, A., Dallinga, J.W., Jonkers, D.M. a. E., Tigchelaar, E.F.,
375 Dekens, J., Zhernakova, A., Ludwig, T., Masclee, A. a. M., Wijmenga, C., van Schooten, F.J.,
376 2016. Volatile organic compounds in breath as markers for irritable bowel syndrome: a
377 metabolomic approach. *Aliment. Pharmacol. Ther.* 44, 45–56. doi:10.1111/apt.13654
- 378 Bean, H.D., Rees, C.A., Hill, J.E., 2016. Comparative analysis of the volatile metabolomes of
379 *Pseudomonas aeruginosa* clinical isolates. *J. Breath Res.* 10, 047102. doi:10.1088/1752-
380 7155/10/4/047102
- 381 Benjamini, Y., Hochberg, Y., 1995. Controlling the False Discovery Rate: A Practical and Powerful
382 Approach to Multiple Testing. *J. R. Stat. Soc. Ser. B Methodol.* 57, 289–300.
- 383 Brunner, C., Szymczak, W., Höllriegel, V., Mörtl, S., Oelmez, H., Bergner, A., Huber, R.M.,
384 Hoeschen, C., Oeh, U., 2010. Discrimination of cancerous and non-cancerous cell lines by
385 headspace-analysis with PTR-MS. *Anal. Bioanal. Chem.* 397, 2315–2324.
386 doi:10.1007/s00216-010-3838-x
- 387 Buuren, S. van, Groothuis-Oudshoorn, K., 2011. mice: Multivariate Imputation by Chained Equations
388 in R. *J. Stat. Softw.* 45, 1–67.
- 389 Diliberto, E.J., Axelrod, J., 1976. Regional and Subcellular Distribution of Protein Carboxymethylase
390 in Brain and Other Tissues. *J. Neurochem.* 26, 1159–1165. doi:10.1111/j.1471-
391 4159.1976.tb07001.x
- 392 Diliberto, E.J., Axelrod, J., 1974. Characterization and substrate specificity of a protein
393 carboxymethylase in the pituitary gland. *Proc. Natl. Acad. Sci.* 71, 1701–1704.
- 394 Dorokhov, Y.L., Shindyapina, A.V., Sheshukova, E.V., Komarova, T.V., 2015. Metabolic Methanol:
395 Molecular Pathways and Physiological Roles. *Physiol. Rev.* 95, 603–644.
396 doi:10.1152/physrev.00034.2014
- 397 Farneti, B., Di Guardo, M., Khomenko, I., Cappellin, L., Biasioli, F., Velasco, R., Costa, F., 2017.
398 Genome-wide association study unravels the genetic control of the apple volatilome and its
399 interplay with fruit texture. *J. Exp. Bot.* doi:10.1093/jxb/erx018
- 400 Fernández del Río, R., O'Hara, M.E., Holt, A., Pemberton, P., Shah, T., Whitehouse, T., Mayhew,
401 C.A., 2015. Volatile Biomarkers in Breath Associated With Liver Cirrhosis — Comparisons
402 of Pre- and Post-liver Transplant Breath Samples. *EBioMedicine* 2, 1243–1250.
403 doi:10.1016/j.ebiom.2015.07.027
- 404 Filipiak, W., Filipiak, A., Sponring, A., Schmid, T., Zelger, B., Ager, C., Ewa Klodzinska, Denz, H.,
405 Pizzini, A., Lucciarini, P., Jammig, H., Troppmair, J., Amann, A., 2014. Comparative analyses
406 of volatile organic compounds (VOCs) from patients, tumors and transformed cell lines for
407 the validation of lung cancer-derived breath markers. *J. Breath Res.* 8, 027111.
408 doi:10.1088/1752-7155/8/2/027111
- 409 Filipiak, W., Mochalski, P., Troppmair, J., Unterkofler, K., Agapiou, A., Davis, C., Cumeras, R.,
410 Ager, C., Filipiak, A., 2016. A compendium of volatile organic compounds (VOCs) released
411 by human cell lines. *Curr. Med. Chem.* 23, 1–1. doi:10.2174/0929867323666160510122913
- 412 Fiserova-Bergerova, V., 1985. Toxicokinetics of organic solvents. *Scand. J. Work. Environ. Health* 11
413 Suppl 1, 7–21.
- 414 Fiserova-Bergerova, V., Diaz, M.L., 1986. Determination and prediction of tissue-gas partition
415 coefficients. *Int. Arch. Occup. Environ. Health* 58, 75–87.
- 416 Fuchs, H., Gailus-Durner, V., Adler, T., Pimentel, J.A.A., Becker, L., Bolle, I., Brielmeier, M.,
417 Calzada-Wack, J., Dalke, C., Ehrhardt, N., Fasnacht, N., Ferwagner, B., Frischmann, U.,
418 Hans, W., Hölter, S.M., Hölzlwimmer, G., Horsch, M., Javaheri, A., Kallnik, M., Kling, E.,
419 Lengger, C., Maier, H., Mossbrugger, I., Mörth, C., Naton, B., Nöth, U., Pasche, B., Prehn,

1
2
3
4
5
6
7
8
9
10
11
12
13
14
15
16
17
18
19
20
21
22
23
24
25
26
27
28
29
30
31
32
33
34
35
36
37
38
39
40
41
42
43
44
45
46
47
48
49
50
51
52
53
54
55
56
57
58
59
60

- C., Przemeck, G., Puk, O., Racz, I., Rathkolb, B., Rozman, J., Schäble, K., Schreiner, R., Schrewe, A., Sina, C., Steinkamp, R., Thiele, F., Willershäuser, M., Zeh, R., Adamski, J., Busch, D.H., Beckers, J., Behrendt, H., Daniel, H., Esposito, I., Favor, J., Graw, J., Heldmaier, G., Höfler, H., Ivandic, B., Katus, H., Klingenspor, M., Klopstock, T., Lengeling, A., Mempel, M., Müller, W., Neschen, S., Ollert, M., Quintanilla-Martinez, L., Rosenstiel, P., Schmidt, J., Schreiber, S., Schughart, K., Schulz, H., Wolf, E., Wurst, W., Zimmer, A., Hrabě de Angelis, M., 2009. The German Mouse Clinic: a platform for systemic phenotype analysis of mouse models. *Curr. Pharm. Biotechnol.* 10, 236–243.
- Hooper, L.V., Gordon, J.I., 2001. Commensal Host-Bacterial Relationships in the Gut. *Science* 292, 1115–1118. doi:10.1126/science.1058709
- Horton, V.L., Higuchi, M.A., Rickert, D.E., 1992. Physiologically based pharmacokinetic model for methanol in rats, monkeys, and humans. *Toxicol. Appl. Pharmacol.* 117, 26–36.
- Hüppe, T., Lorenz, D., Maurer, F., Albrecht, F.W., Schnauber, K., Wolf, B., Sessler, D.I., Volk, T., Fink, T., Kreuer, S., 2016. Exhalation of volatile organic compounds during hemorrhagic shock and reperfusion in rats: an exploratory trial. *J. Breath Res.* 10, 016016. doi:10.1088/1752-7155/10/1/016016
- Kistler, M., Muntean, A., Szymczak, W., Rink, N., Fuchs, H., Valerie Gailus-Durner, Wurst, W., Hoeschen, C., Klingenspor, M., Angelis, M.H. de, Jan Rozman, 2016. Diet-induced and mono-genetic obesity alter volatile organic compound signature in mice. *J. Breath Res.* 10, 016009. doi:10.1088/1752-7155/10/1/016009
- Kistler, M., Szymczak, W., Fedrigo, M., Fiamoncini, J., Höllriegel, V., Hoeschen, C., Klingenspor, M., Hrabě de Angelis, M., Rozman, J., 2014. Effects of diet-matrix on volatile organic compounds in breath in diet-induced obese mice. *J. Breath Res.* 8, 016004. doi:10.1088/1752-7155/8/1/016004
- Lindinger, W., Taucher, J., Jordan, A., Hansel, A., Vogel, W., 1997. Endogenous Production of Methanol after the Consumption of Fruit. *Alcohol. Clin. Exp. Res.* 21, 939–943. doi:10.1111/j.1530-0277.1997.tb03862.x
- Nakhleh, M.K., Amal, H., Jeries, R., Broza, Y.Y., Aboud, M., Gharra, A., Ivgi, H., Khatib, S., Badarneh, S., Har-Shai, L., Glass-Marmor, L., Lejbkowitz, I., Miller, A., Badarny, S., Winer, R., Finberg, J., Cohen-Kaminsky, S., Perros, F., Montani, D., Girerd, B., Garcia, G., Simonneau, G., Nakhoul, F., Baram, S., Salim, R., Hakim, M., Gruber, M., Ronen, O., Marshak, T., Doweck, I., Nativ, O., Bahouth, Z., Shi, D., Zhang, W., Hua, Q., Pan, Y., Tao, L., Liu, H., Karban, A., Koifman, E., Rainis, T., Skapars, R., Sivins, A., Ancans, G., Liepniece-Karele, I., Kikuste, I., Lasina, I., Tolmanis, I., Johnson, D., Millstone, S.Z., Fulton, J., Wells, J.W., Wilf, L.H., Humbert, M., Leja, M., Peled, N., Haick, H., 2016. Diagnosis and Classification of 17 Diseases from 1404 Subjects via Pattern Analysis of Exhaled Molecules. *ACS Nano.* doi:10.1021/acsnano.6b04930
- Obermeier, J., Trefz, P., Happ, J., Schubert, J.K., Staude, H., Fischer, D.-C., Miekisch, W., 2017. Exhaled volatile substances mirror clinical conditions in pediatric chronic kidney disease. *PloS One* 12, e0178745. doi:10.1371/journal.pone.0178745
- O'Hara, M.E., Clutton-Brock, T.H., Green, S., Mayhew, C.A., 2009. Endogenous volatile organic compounds in breath and blood of healthy volunteers: examining breath analysis as a surrogate for blood measurements. *J. Breath Res.* 3, 027005. doi:10.1088/1752-7155/3/2/027005
- Paterson, S., Mackay, D., 1989. Correlation of tissue, blood, and air partition coefficients of volatile organic chemicals. *Br. J. Ind. Med.* 46, 321–328.
- Pleil, J.D., Stiegel, M.A., Risby, T.H., 2013. Clinical breath analysis: discriminating between human endogenous compounds and exogenous (environmental) chemical confounders. *J. Breath Res.* 7, 017107. doi:10.1088/1752-7155/7/1/017107
- Puchalska, P., Crawford, P.A., 2017. Multi-dimensional Roles of Ketone Bodies in Fuel Metabolism, Signaling, and Therapeutics. *Cell Metab.* 25, 262–284. doi:10.1016/j.cmet.2016.12.022
- Ruzsanyi, V., Lederer, W., Seger, C., Calenic, B., Liedl, K.R., Amann, A., 2014. Non-13CO₂ targeted breath tests: a feasibility study. *J. Breath Res.* 8, 046005. doi:10.1088/1752-7155/8/4/046005

- 1
2
3 473 Sinues, P.M.-L., Kohler, M., Brown, S.A., Zenobi, R., Dallmann, R., 2017. Gauging circadian
4 474 variation in ketamine metabolism by real-time breath analysis. *Chem. Commun.* 53, 2264–
5 475 2267. doi:10.1039/C6CC09061C
6
7 476 Skrzydlewska, E., 2003. Toxicological and Metabolic Consequences of Methanol Poisoning. *Toxicol.*
8 477 *Mech. Methods* 13, 277–293. doi:10.1080/713857189
9 478 Španěl, P., Dryahina, K., Vicherková, P., Smith, D., 2015. Increase of methanol in exhaled breath
10 479 quantified by SIFT-MS following aspartame ingestion. *J. Breath Res.* 9, 047104.
11 480 doi:10.1088/1752-7155/9/4/047104
12 481 Sweeting, J.N., Siu, M., McCallum, G.P., Miller, L., Wells, P.G., 2010. Species differences in
13 482 methanol and formic acid pharmacokinetics in mice, rabbits and primates. *Toxicol. Appl.*
14 483 *Pharmacol.* 247, 28–35. doi:10.1016/j.taap.2010.05.009
15 484 Szymczak, W., Rozman, J., Höllriegel, V., Kistler, M., Keller, S., Peters, D., Kneipp, M., Schulz, H.,
16 485 Hoeschen, C., Klingenspor, M., de Angelis, M.H., 2014. Online breath gas analysis in
17 486 unrestrained mice by hs-PTR-MS. *Mamm. Genome Off. J. Int. Mamm. Genome Soc.* 25,
18 487 129–140. doi:10.1007/s00335-013-9493-8
19
20 488 van Vliet, D., Smolinska, A., Jöbsis, Q., Rosias, P., Muris, J., Dallinga, J., Dompeling, E., van
21 489 Schooten, F.-J., 2017. Can exhaled volatile organic compounds predict asthma exacerbations
22 490 in children? *J. Breath Res.* 11, 016016. doi:10.1088/1752-7163/aa5a8b
23 491 Ward, K.W., Blumenthal, G.M., Welsch, F., Pollack, G.M., 1997. Development of a physiologically
24 492 based pharmacokinetic model to describe the disposition of methanol in pregnant rats and
25 493 mice. *Toxicol. Appl. Pharmacol.* 145, 311–322. doi:10.1006/taap.1997.8170
26 494 Wickham, H., 2009. *ggplot2: elegant graphics for data analysis*. <http://had.co.nz/ggplot2/book>.
27 495 Springer New York.
28 496
29
30
31
32
33
34
35
36
37
38
39
40
41
42
43
44
45
46
47
48
49
50
51
52
53
54
55
56
57
58
59
60